Journal of Materials Chemistry

Cite this: *J. Mater. Chem.*, 2012, **22**, 19438

www.rsc.org/materials

PAPER

GAGs-thiolated chitosan assemblies for chronic wounds treatment: control of enzyme activity and cell attachment

Antonio Francesko,[a] Diana Soares da Costa,[bc] Patrícia Lisboa,[bc] Rui L. Reis,[bc] Iva Pashkuleva[bc] and Tzanko Tzanov*[a]

Received 20th February 2012, Accepted 20th April 2012
DOI: 10.1039/c2jm31051a

Multilayered polyelectrolyte coatings comprising thiolated chitosan (TC) and glycosaminoglycans (GAGs), chondroitin sulphate and hyaluronic acid, were built using a layer-by-layer approach. The surface activity of these coatings for binding and inhibition of enzymes related to chronic inflammation, such as collagenase and myeloperoxidase, was assessed. The build-up of five bi-layers of TC/GAGs onto gold surfaces was monitored *in situ* by QCM-D. All experimental groups showed exponential growth of the coatings controlled by the degree of chitosan thiolation and the molecular weight of the GAGs. The degree of chitosan modification was also the key parameter influencing the enzyme activity: increasing the thiols content led to more efficient myeloperoxidase inhibition and was inversely proportional to the adsorption of collagenase. Enhanced fibroblast attachment and proliferation were observed when the multilayered polyelectrolyte constructs terminated with GAGs. The possibility to control either the activity of major wound enzymes by the thiolation degree of the coating or the cell adhesion and proliferation by proper selection of the ultimate layer makes these materials potentially useful in chronic wounds treatment and dermal tissue regeneration.

Introduction

Chronic wounds arise upon the disruption of the acute wound healing process usually expressed at the inflammatory stage. They are characterised by an imbalance between production and degradation of extracellular matrix (ECM) components in favour of degradation. The excessive degradation is the result of the simultaneous action of proteolytic enzymes, such as matrix metalloproteinase (MMPs), at the wound site.[1,2] Examples of MMPs are collagenases that specifically recognise and cleave collagen – the main protein in connective tissues and skin. Prolonged inflammation also leads to the accumulation of neutrophils in the wound that undergo apoptosis and release their constituents such as oxidative enzymes. Hypochlorous acid (HOCl), generated by the main neutrophil enzyme – myeloperoxidase (MPO), together with other reactive oxygen species (ROS) oxidises most biological molecules, including the protease inhibitors, thereby promoting proteolytic damage of the tissue.[3] It is believed that by bringing the activity levels of major chronic wound enzymes down to the levels found in healing wounds the balance between molecule degradation and production can be restored, which may then allow healing to progress.[4]

Most of the approaches for chronic wounds management are based on the topical application or the release of active compounds from the dressing platforms into the wound.[5] Despite some of the approaches including controlled release of active agents[6] the biggest concern, however, remains the side effects due to the accumulation of immunoreactive compounds at the wound site,[7] *i.e.* overdoses. The permanent immobilisation of the active agents on the surface of the dressing would prevent overdoses in clinical application. Nowadays, the modification of surfaces is a key aspect in biotechnology including development of substrates for regenerative medicine.[8] By alteration of the surface functionality controlled chemical and biological interactions can be achieved.[9] The objective of this work was to develop a functional coating able to control the activities of deleterious chronic wound enzymes through specific surface interactions for promoting the wound healing process. Since the control of MMP activity can be achieved by redox-regulation of cysteine residue coordinating Zn^{2+} at the enzyme active site,[10] or directly by metal chelation, thiol groups that combine both functions,[11] and in addition inhibit human MPO,[12] were incorporated in chitosan (Chi). The functionalised chitosan (TC) was then used to build polyelectrolyte multilayered (PEM) structures by assembling with the glycosaminoglycans (GAGs), chondroitin sulphate (CS) and hyaluronic acid (HA), as counterions. The preparation of such assemblies through the

[a]*Group of Molecular and Industrial Biotechnology, Department of Chemical Engineering, Universitat Politècnica de Catalunya, Passeig Ernest LLuch/Rambla Sant Nebridi s/n, 08222 Terrassa, Spain. E-mail: tzanko.tzanov@upc.edu; Fax: +34 937398225; Tel: +34 937398570*
[b]*3B's Research Group - Biomaterials, Biodegradables and Biomimetics, University of Minho, Headquarters of the European Institute of Excellence on Tissue Engineering and Regenerative Medicine, AvePark, 4806-909 Taipas, Guimarães, Portugal. E-mail: pashkuleva@dep.uminho.pt; Fax: +351 253 510909; Tel: +351 253 510907*
[c]*ICVS/3B's - PT Government Associate Laboratory, Braga/Guimarães, Portugal*

layer-by-layer approach is a convenient technique to functionalise a surface to impart specific surface bio-activity towards various bioentities, *e.g.* proteins and cells.[13,14] From a technological point of view, the alternate deposition of oppositely charged polymers represents a simple approach for surface modification, while rendering it suitable for the interaction with biological tissues in a relatively predictable way.[15] Control of the physicochemical and biological properties of multilayer coatings/films can be achieved by adjusting the process parameters such as pH, layer number, cross-linking and nature of the outermost layer.[16] In this work the capacity of the obtained multilayered assemblies for inhibition and/or adsorption of major wound enzymes, namely MPO and collagenase, was evaluated *in vitro*. Build-up of the coatings onto gold surfaces and adsorption behaviour of collagenase as a function of the nature of the outermost layer were assessed *in situ* by quartz crystal microbalance with dissipation (QCM-D). The importance of the outermost layer was also investigated in terms of fibroblasts adhesion and proliferation.

Materials and methods

2-Iminothiolane HCl, *N*-[3-(2-furyl)acryloyl]-Leu-Gly-Pro-Ala (FALGPA) and collagenase from *Clostridium histolyticum* (0.27 U mg^{-1} solid, one unit hydrolyses 1.0 μmol of FALGPA per minute at pH 7.5 and 25 °C in the presence of calcium ions) were purchased from Sigma-Aldrich. Purified MPO from human leukocytes (1550 U mg^{-1} solid, one unit produces an increase in absorbance at 470 nm of 1.0 per min at pH 7.0 and 25 °C, calculated from the initial rate of reaction using guaiacol substrate) was from Planta Natural Products (Austria). All other reagents and buffers were of analytical grade purchased from Sigma-Aldrich, unless specified otherwise, and used as received.

Being natural components of the ECM, GAGs were selected as building elements for PEM coatings. They are also capable of absorbing excessive wound exudates while still providing favourable moist environment for wound healing. Previous reports[17,18] have demonstrated that both sulphated and non-sulphated (hyaluronic acid) GAGs accelerate acute wound healing. In this work sodium hyaluronate with different M_w (6 kDa, 830 kDa and 2000 kDa, $pK_a \approx 3$, ref. 19) from Lifecore Biomedical (USA) and the sodium salt of chondroitin sulphate (~20 kDa, DS 0.9, $pK_a \approx 3.5$ for higher ionic strengths[20]) kindly supplied by Innovent (Germany) were used.

Chitosan has a similar structure to the natural GAGs but it bears a positive charge allowing assembly *via* electrostatic interactions with the negatively charged GAGs. Moreover, it has been employed for the construction of a wide variety of wound healing devices because of its intrinsic antimicrobial properties and ability to accelerate healing by increasing the rate of infiltration of fibroblasts at the wound site and consequentially the collagen production.[21] Therefore, medical grade chitosan (~50 kDa, DDA 87%, $pK_a \approx 6.5$, ref. 22) from Kitozyme (Belgium) was used for further thiolation. Thiol-modified polymers have been already exploited for inhibition of some metal-dependent enzymes.[23]

Chitosan thiolation and characterisation

The synthesis of thiolated chitosan was carried out in a one-step coupling reaction between 2-iminothiolane HCl and primary amino groups of chitosan, according to Bernkop-Schnürch *et al.*[24] Batches differing in the thiolation degree were prepared by altering the amount of the coupling reagent in the reaction mixture and the thiolated conjugates were designated accordingly (Table 1).

Sulphur elemental analysis (EuroVector 3011 CHNS Elemental Analyzer, Italy) was performed to determine the total sulphur content. The amount of reduced thiol groups was determined spectrophotometrically using Ellman's reagent.[25]

Enzymes assays

The inhibitory effect of thiolated chitosan on MPO activity was measured spectrophotometrically using guaiacol as a substrate.[26] Samples (2 mg) were incubated with MPO and guaiacol buffered with 50 mM PBS, pH 6.6 at 37 °C for 1 h. Thereafter, the reaction was initiated by adding H_2O_2. The final assay concentrations were: 0.24 U MPO, 10 mM guaiacol and 1 mM H_2O_2. The activity was determined by the increase of the absorbance rate (470 nm) per min and expressed as a percentage of MPO inhibition compared to the non-modified chitosan control. All assays were performed in triplicate.

The collagenase activity was measured as described by Van Wart and Steinbrink.[27] The hydrolysis of FALGPA (1 mM) by collagenase (0.2 μg mL^{-1}) in the presence of thiolated chitosan in 50 mM Tricine (pH 7.5) containing 100 mM $CaCl_2$ and 400 mM NaCl was monitored at 345 nm.

Layer-by-layer assembly of PEM coatings and collagenase adsorption

Solutions of chitosan, thiolated conjugates and glycosaminoglycans (0.5 mg mL^{-1}) containing NaCl (0.15 M) were prepared, and the pH adjusted to 5.5 with HCl or NaOH solutions. The ζ-potential of each solution was determined at 25 °C (Nano-ZS from Malvern, UK). The deposition of the polyelectrolytes was carried out at the same temperature and at a constant flow rate (75 μL min^{-1}) onto the surface of Au coated sensor crystals (Q-Sense, Sweden). The crystals were first cleaned with H_2O_2 (30%)–NH_4OH (25%)–H_2O (1 : 1 : 5) for 10 min at 75 °C. The process was followed *in situ* by quartz crystal microbalance with dissipation (QCM-D, E4 system from Q-Sense, Sweden). The baseline was built using a 0.15 M NaCl solution. Different multilayered systems were built by consecutive depositions of polycation (Chi, TC10-1 or TC5-2, Table 1) and polyanion (HA with different molecular weights or CS) solutions. The solutions were injected into the measurement chamber for 10 min followed by a rinsing step (10 min) with 0.15 M NaCl, pH 5.5. This procedure was repeated 5 times to obtain five bi-layer substrates. Collagenase (0.1 mg mL^{-1} in 0.15 M NaCl, pH 5.5) deposition was monitored *in situ* by QCM-D for 3 h at a constant flow of 10 μL min^{-1}. At the end of this time a rinsing step with a protein-free solution was applied (1 h) to remove weakly adsorbed and unadsorbed proteins. Each study was performed in triplicate. For graphical simplification the evolutions of the normalised frequency ($\Delta f/\nu$) and dissipation (ΔD) shifts as functions of time of one representative per experimental group and only for the 9th harmonic are shown. Coating growth (thickness variation) as a function of the layer number and the amount of collagenase

Table 1 Total sulphur content, percentage of free thiol groups, and disulphide content in the obtained thiolated chitosan conjugates

Sample	Chi : 2-iminothiolane HCl (w/w)	Total sulphur content (%, w/w)	Free thiol groups (% of total S)	S–S (% of total S)
Chitosan	—	—	—	—
TC10-1	10 : 1	2.08	61	39
TC5-1	5 : 1	3.61	69	31
TC5-2	5 : 2	5.43	60	40
TC2-1	2 : 1	5.82	57	43

adsorbed on coatings was estimated using the Voigt model (Q-Tools software, Q-Sense). By using this model the values for the coating thickness obtained for the first layer adsorption are usually non-reproducible, therefore these values were excluded from the data.[28]

Characterisation of PEM coatings

The PEM coatings were characterised by X-ray photoelectron spectroscopy and contact angle measurements. Multilayered systems were deposited on Au coated (100 Å) glass microscopy slides (Sigma-Aldrich) cut into pieces of 1 cm^2 and cleaned using the same protocol as the one described for QCM crystals. A custom-made dipping robot was used for the biopolymers deposition. The assembling process was performed using the same conditions (solution concentration, pH, ionic strength and deposition/rinsing times) described above. Multilayered systems differing in the layer number (1, 3, 7 and 11) and composition of the outermost layer were prepared.

X-ray photoelectron spectroscopy (XPS)

XPS analyses were performed on a PHI 5500 Multitechnique System (Physical Electronics, USA) using a monochromatic Al-Kα X-ray source ($h\nu$ 1486.6 eV), placed perpendicularly to the analyser axis and calibrated using the 3d5/2 line of Ag with a full width at half maximum (FWHM) of 0.8 eV. The analysed area was a circle of 0.8 mm diameter, and the resolution chosen for the spectra was 187.5 eV of pass energy and 0.8 eV per step for survey spectra, and 0.1 eV per step for each analysed element. Binding energies were referenced by setting the Au4f7/2 at 84.0 eV. Surface elemental composition was determined using the standard Scofield photoemission cross-sections.

Contact angle measurements

The hydrophilicity of the PEM coatings prepared on the Au coated glass microscopy slides was assessed by means of static contact angle measurements (sessile drop method) with ultrapure water, using drop shape analysis system DSA 100, Kruss, GmbH (Germany), equipped with a ½ inch CCD camera. The volume of the liquid droplet was 5 µL. Ten measurements at room temperature were taken for each sample.

Cell adhesion, proliferation and morphology

PEM coatings of 5 and 5½ bi-layers were sterilised by UV radiation for 15 min and washed with phosphate buffered saline (PBS). The substrates were seeded with L929 human fibroblast-like cell line (European Collection of Cell Cultures, UK) at a concentration of 16 500 cells per cm^2 in Dulbecco's modified eagle's medium (DMEM) supplemented with 10% fetal bovine serum (FBS, Biochrom AG, Germany) and 1% antibiotic/antimycotic (Gibco, USA). Cells were cultured for 1 and 7 days at 37 °C under a humidified atmosphere of 5% CO_2.

The morphology of the cells was observed by scanning electron microscopy (SEM, Leica Cambridge S-360, 15 kV) and fluorescence microscopy (Zeiss Imager Z1, Germany). The samples were washed twice with PBS and fixed either in 2.5% glutaraldehyde in PBS (for SEM) or in 10% neutral buffered formalin for 1 h at 4 °C for immunostaining assays. For the SEM analysis, samples were washed twice in PBS, dehydrated in a graded series of ethanol, and finally, dried using hexamethyldisilazane. Cytoskeleton organization was analysed after treatment of the cells with 0.2% Triton X-100 in PBS for 5 min and 3% BSA in PBS for 30 min at room temperature. Phalloidin–TRITC conjugate was used (1 : 200 in PBS for 30 min) to assess cytoskeleton organisation. Nuclei were counterstained with 1 µg mL^{-1} 4,6-diamidina-2-phenylin (DAPI) for 30 min. Samples were washed with PBS, mounted with Vectashield® (Vector) in glass slides and images were acquired with an Axio Cam MRm (Zeiss).

Statistical analysis

All data are presented as mean ± standard deviation (SD). For multiple comparisons, statistical analysis by a one way analysis of variance (ANOVA) followed by the *post-hoc* Tukey test was performed using Graph Pad Prism Software 5.04 for windows (USA). Statistical significance was considered at $p < 0.01$.

Results and discussion

Thiolated chitosan

Thiolated chitosan conjugates were obtained in a one-step coupling reaction between 2-iminothiolane HCl and primary amino groups of the polymer. The expected conjugate structure is shown in Scheme 1.

This reaction allows for the immobilisation of free thiol groups on the chitosan backbone whereas the established amidine linkages provide improved cationic character of chitosan,[29] confirmed by ζ potential measurements (Fig. 1).

The sulphur content in the samples (Table 1) increased with the increase of 2-iminothiolane HCl concentration, demonstrating a successful coupling with chitosan. Between 31 and 43% of the total sulphur content was in the form of disulphide bridges, *i.e.* oxidised during the time-consuming dialysis step of the conjugates preparation.[29]

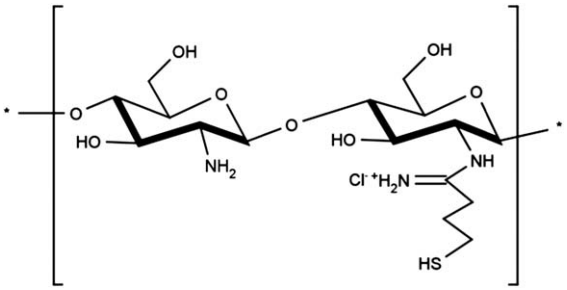

Scheme 1 Proposed structure of the obtained thiolated chitosan conjugates.

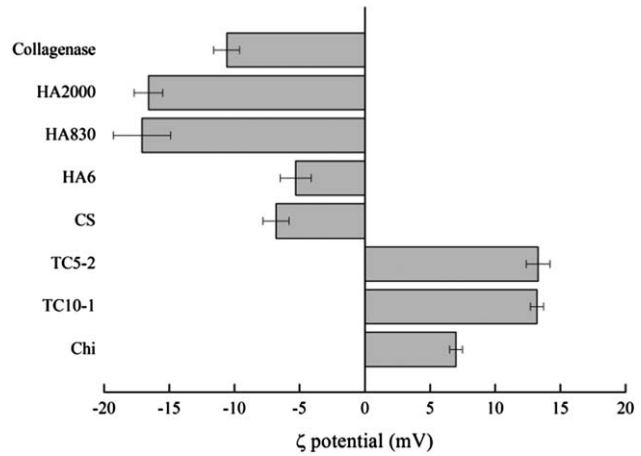

Fig. 1 ζ Potential of collagenase and the polyelectrolytes used for the QCM-D studies. Polyelectrolytes (0.5 mg mL^{-1}) and collagenase (0.1 mg mL^{-1}) solutions were prepared in 0.150 M NaCl, pH 5.5.

Effect of thiolated chitosan on major chronic wound enzyme activities

The identification of elevated levels of oxidative MPO and matrix degrading proteolytic MMPs in chronic wound fluids[1,30] led to a considerable interest for these enzymes as potential therapeutic targets.[31,32] The product of the MPO-induced oxidation of physiological chloride in the presence of H_2O_2 is the potent antimicrobial oxidant hypochlorous acid (HOCl). However, the persistent activity of the MPO–H_2O_2 system may adversely affect the tissues under pathological conditions. The accumulated HOCl is able to oxidatively modify lipids, DNA and (lipo) proteins by halogenation, nitration and oxidative crosslinking. On the other hand, collagenases belong to the family of zinc-proteins able to hydrolyse the triple helical regions of collagen under physiological conditions. As in all MMPs, collagenases possess catalytic Zn^{2+} in the active centre coordinated by a redox-sensitive cysteine residue. In the normal healing process collagenases contribute to the reconstruction of damaged skin. However, their elevated level in chronic wounds causes uncontrolled degradation of newly formed ECM impairing the healing process. It is therefore crucial to maintain MPO and MMPs activity during the host defence (MPO induces HOCl generation needed for the bacterial killing) and reconstruction of ECM (involving collagenases), but interfere with their pathophysiologically persistent activation.

Some collagenase inhibitors bearing Zn^{2+} binding groups attack the zinc site in the catalytic domain of the enzyme.[33] By the same mechanism thiol compounds inhibit collagenases,[22] and in addition have the capacity to inhibit MPO.[7] While some authors reported thiolated polymers as efficient inhibitors of zinc-dependent enzymes through metal chelation,[23] others found that the binding tendency of thiols immobilised onto polymers in solution is not high enough to develop effective ion depletion from the enzymes' active sites, unlike when such systems are applied as coating components due to different polymer chains rearrangement.[34]

The thiolated chitosan conjugates obtained in this work were able to inhibit the activity of MPO in solution (Fig. 2). Moreover, the degree of MPO inhibition can be tuned by the percentage of the chitosan thiolation. On the other hand, no reduction of collagenase activity by thiolated conjugates was found (measured using FALGPA as a substrate; results not shown).

The IC_{50} values for MPO and collagenase inhibition by 2-iminothiolane HCl were 85 ± 2 μM and 24 ± 3 mM, respectively. This large difference indicates that chitosan with much higher thiolation grade is needed to inhibit collagenase in solution and to be detected by the enzymatic assay used. Alternatively, the affinity of collagenase towards surfaces coated with thiolated chitosan was evaluated by QCM-D.

Polyelectrolyte multilayered coatings

Effect of the chitosan thiolation degree on build-up of PEMs. The stepwise adsorption of polyelectrolytes was monitored *in situ* by QCM-D, and the effect of the chitosan thiolation degree and molecular weight of GAGs on the growth of the coatings was assessed. The successful build-up of the PEM constructs using the layer-by-layer process was confirmed by the decrease in $\Delta f/\nu$ and increase of ΔD after each polyelectrolyte deposition (Fig. 3a and b). Bigger changes in $\Delta f/\nu$ and ΔD shifts were observed for the first layer when thiolated chitosan was used as a polycation instead of an unmodified chitosan. This difference was expected

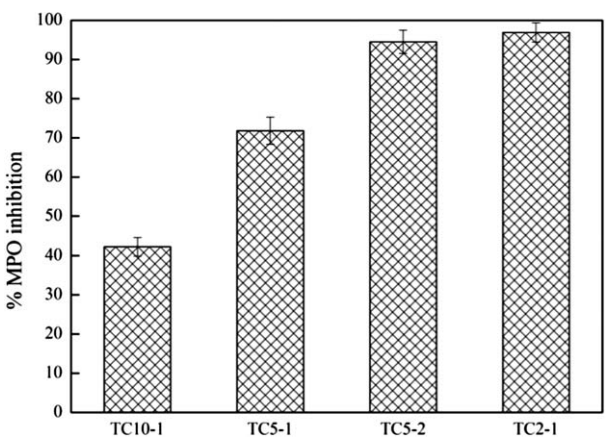

Fig. 2 Effect of thiolated chitosan conjugates on the myeloperoxidase (MPO) activity. Incubation mixture: thiolated chitosan samples (2 mg), myeloperoxidase (0.60 U) and guaiacol (167 mM) in 500 μL of 50 mM PBS, pH 6.6 at 37 °C for 1 h. H_2O_2 final concentration: 1 mM. Enzymatic reaction time: 90 s. The results are shown as mean values for myeloperoxidase inhibition by each experimental group compared to non-modified chitosan control ± standard deviation ($n = 3$).

because of the well-known high affinity of the thiol groups to Au.[35] Changes in $\Delta f/\nu$ and ΔD shifts become more pronounced after the deposition of the 6th layer for all experimental groups and especially for the systems built with thiolated chitosan conjugates. These data indicated an exponential growth confirmed by the calculation of thickness variation using the Voigt model (Fig. 3c). The results imply that polyelectrolytes diffuse "in and out" of the coating during the build-up process.[36] Interestingly, the thickness variation in respect of layer number was higher when thiol-modified compared to non-modified chitosan was used, where the thiolation degree promoted the growth as the final thicknesses for the 5½ bi-layer systems were 27 ± 2 nm, 37 ± 2 nm and 52 ± 5 nm for Chi/CS, TC10-1/CS and TC5-2, respectively. Thus, the improved cationic character after chitosan thiolation with 2-iminothiolane HCl (Fig. 1) induces stronger electrostatic interactions with chondroitin sulphate and together with better deposition of the first layer favours the PEM coating growth.

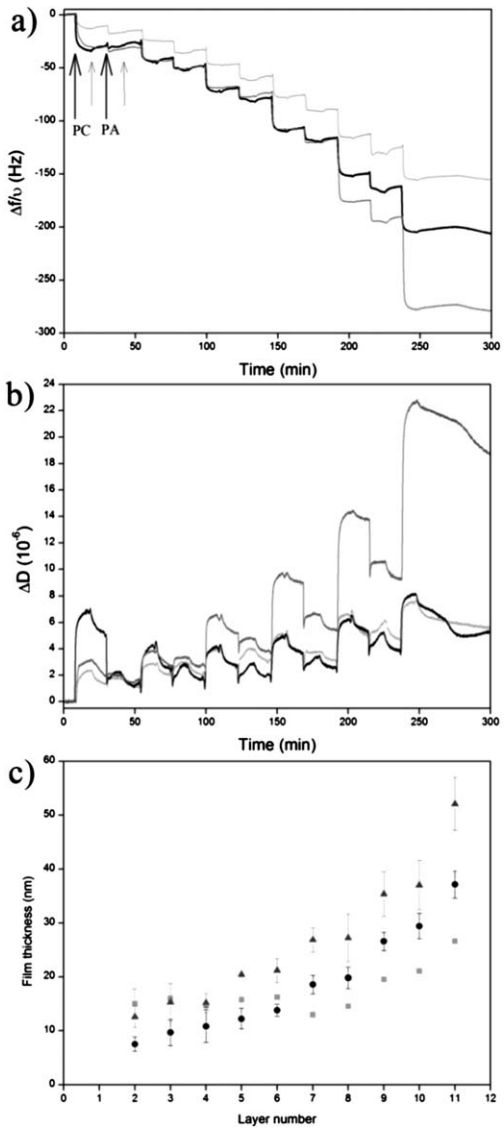

Fig. 3 Build-up assessments of 5½ bi-layers of Chi/CS (light grey), TC10-1/CS (black) and TC5-2/CS (dark grey). Signals for normalized (a) frequency ($\Delta f/\nu$) and (b) dissipation (ΔD) were obtained during QCM-D monitoring. Labelled arrows indicate polyelectrolyte injection (PC for polycation, PA for polyanion), whereas small arrows without labels indicate rinsing with 0.15 M NaCl, pH 5.5. (c) Thickness evolution of the obtained PEMs estimated using the Voigt model for three independent experiments.

Finally, although the stability of the PEM coatings was not investigated here, the partial oxidation of the free thiol groups leads to the formation of cross-links in chitosan[37] that would certainly improve the mechanical properties of the systems and enhance their stability in biological fluids. Chemical cross-linking has been already investigated as an approach to increase the stability of PEMs[38] and improve their mechanical properties.[39]

Effect of molecular weight of glycosaminoglycans on build-up of PEMs. QCM-D experiments were also conducted to investigate the effect of M_w of polyanion on the build-up of multilayered coatings containing thiolated chitosan. HA with three molecular weights (6 kDa, 830 kDa and 2000 kDa) was used for building multilayered systems with TC5-2 (Fig. 4a and b).

Initially, the PEMs grew regularly for all experimental groups. However, the system containing HA with the lowest M_w becomes unstable after the addition of the 8th layer; re-dissolution of the formed complex upon the contact with the following polyelectrolyte solution was observed. A similar effect has been previously observed for other weak PEMs.[38] Although the negative charge of HA with a M_w of 6 kDa was similar to the one of CS (Fig. 1), in the latter case a stable complex with polycation was formed. An efficient GAGs-biomolecules binding relies on multivalent interactions or the so-called cluster effect.[40] Out of this, two are the possible reasons for the results observed with the low M_w HA: the unavailability of enough reaction centres (because of the lower M_w) or their inadequate distribution, *i.e.* their conformation does not allow effective binding through the cluster effect. Thus, we can speculate that CS takes a conformation favouring the interactions with TC which is not the case with low molecular weight HA. In addition, previous reports stating M_w plays an important role for efficient immobilisation of sugars onto many surfaces, where oligosaccharides and monosaccharides cannot be densely and stably immobilised if they are not coupled to larger moieties, support this result.[41,42] Thus, the M_w of 6 kDa is too low to allow for sufficient deposition onto the oppositely charged surface and when the amounts of the deposited polyelectrolytes increase (after the 8th layer) re-dissolution occurs.

The PEM coatings containing HA of higher average molecular weight displayed higher stability and grew exponentially (Fig. 4c); $\Delta f/\nu$ and ΔD shifts became more pronounced after the deposition of the 6th layer. A slightly larger increase was detected for HA of 830 kDa compared to 2000 kDa, due to the better diffusion of the HA with lower M_w into the coating, which is in a good agreement with the literature data for the exponentially growing PEM systems.[43] The calculated thicknesses were 32 ± 2 nm, 113 ± 5 nm and 100 ± 4 nm for PEMs with HA of 6 kDa, 830 kDa and 2000 kDa, respectively. These results confirm the instability of the PEM system build up with low molecular weight HA.

XPS analysis

XPS measurements were performed to confirm the successful deposition of the polyelectrolytes. From the measurements it was

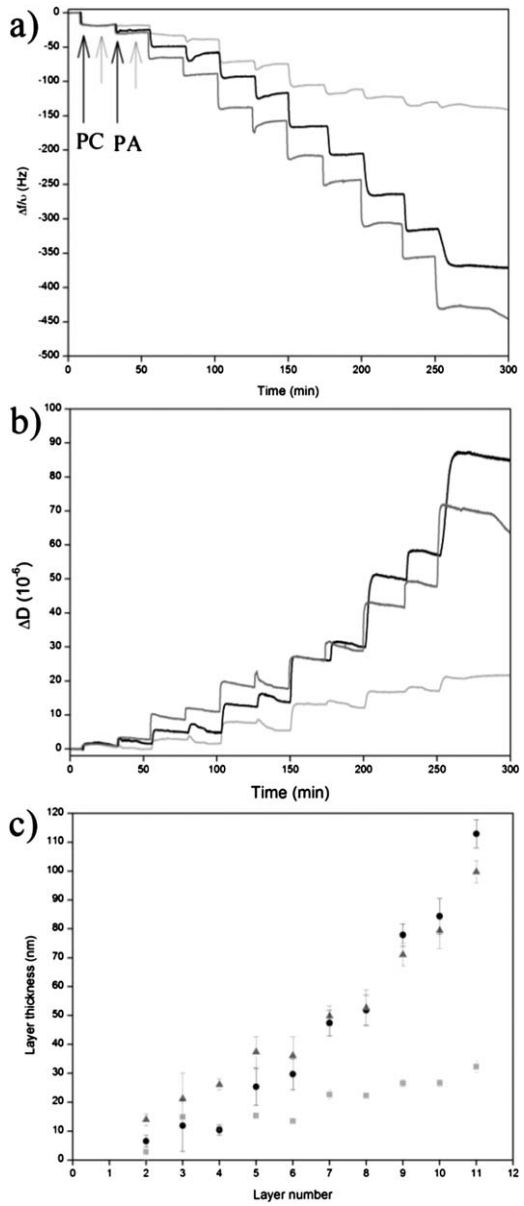

Fig. 4 Build-up assessments of 5½ bi-layers of TC5-2/HA using hyaluronic acid with different M_w: 6 kDa (light grey), 830 kDa (black) and 2000 kDa (dark grey). Signals for normalized (a) frequency ($\Delta f/\nu$) and (b) dissipation (ΔD) were obtained during QCM-D monitoring. Labelled arrows indicate polyelectrolyte injection (PC for polycation, PA for polyanion), whereas small arrows without labels indicate rinsing with 0.15 M NaCl, pH 5.5. (c) Thickness evolution of the obtained PEMs estimated using the Voigt model for three independent experiments.

possible to estimate the surface coverage by analysing Au atomic concentrations at the different steps of deposition (Table 2). As could be expected, the XPS analysis showed a steady decrease in the intensity of the Au signal with increasing number of deposited layers.

The obtained value for Au signal (16.19%) after the deposition of the first layer is in agreement with previously reported values for monolayers of thiolated polymers deposited onto gold surfaces.[44] After 5½ bi-layers deposition of the TC/HA830 system only a negligible Au signal was detected (0.08%). This

Table 2 Au and S contents (%) for various multilayered systems deposited onto gold covered microscopy slides

System	Au (4f)	S (2p)
Gold surface	99.99[a]	—
TC5-2	16.19	1.37
$(TC5\text{-}2/HA830)_1TC5\text{-}2$	1.97	1.66
$(TC5\text{-}2/HA830)_3TC5\text{-}2$	0.18	1.42
$(TC5\text{-}2/HA830)_5TC5\text{-}2$	0.08	1.60
$(Chi/HA830)_5Chi$	0.12	—

[a] According to the manufacturer.

value was lower than the one measured for the Chi/HA830 system for the same number of deposited bi-layers (0.12%) which is in agreement with QCM-D results confirming better build-up and surface coverage for the PEMs containing thiolated compared to the non-modified chitosan.

The presence of S was also observed for all PEMs terminating with TC5-2, where the signal did not vary considerably between the experimental groups (Table 2). The binding energies and the possible oxidation states of S in the TC5-2 deposited on the gold were obtained from the high resolution XPS spectra of the S2p core level. The S2p high resolution spectrum (not presented) showed two dominant peaks at 162.4 eV and 163.6 eV that are assigned to bound S atoms (S2p3/2 and S2p1/2) on the Au surface (thiols and disulphides). Two additional peaks appear in the spectrum of multilayered (5½ bi-layers) TC5-2/HA830 system (Fig. 5). An intensive peak at 164.3 eV corresponding to unbound thiols and a lower intensity peak at above 168 eV due to the partial sulphur oxidation or presence of impurities in the sample[44] were detected. These values were in agreement with literature data.[35,45]

Collagenase adsorption on PEM coatings

Coating of surfaces through PEM deposition has been extensively investigated as a way to rule the protein attachment on

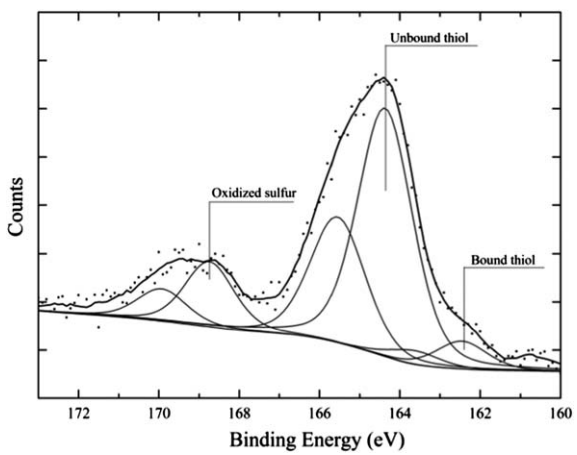

Fig. 5 S2p spectrum of the TC5-2/HA830 multilayer system consisting of 5½ bi-layers adsorbed onto the gold surface acquired by XPS. Polyelectrolytes were deposited onto gold from 0.15 M NaCl, pH 5.5 solution, using concentrations of 0.5 mg mL^{-1}. The S peaks were fit using three S2p doublets with a 2 : 1 area ratio and a splitting of 1.2 eV. The positions of the S2p3/2 peaks assigned to bound thiolate, unbound thiol and oxidized S species are shown.

such surfaces required for different applications and controlled attachment could be achieved by changing an ambient pH, system cross-linking and selection of the outermost layer.[28,46] Moreover, the incorporation of the proteins can be further controlled by an appropriate functionalisation of the PEM components before or even after their construction.[47] As one of the efficient ways to inactivate the proteases at the wound environment is through the selective or non-selective protein adsorption,[48,49] the PEM coatings prepared in this study have been evaluated for their capacity to adsorb collagenase from solution. The effect of chitosan thiolation and the charge of the outermost layer have been considered as variables.

The amount of collagenase adsorption onto PEMs with different terminate layers is shown in Fig. 6. The adsorption was performed at pH 5.5, the same as the one applied in the process of PEMs build-up. This pH was chosen to ensure the optimum protein adsorption since it is near to the isoelectric point of collagenase (p*I* in the range 5.35–6.20, ref. 50) and thus, minimal lateral interactions and compact conformation of protein onto the surface occur.[51] The collagenase is negatively charged under these conditions (Fig. 1) and has higher affinity to positively charged chitosan surfaces regardless of chitosan modification. These results confirmed the dominant role of the electrostatic interactions during protein adsorption.[13,52]

Besides electrostatic interactions, the affinity of chitosan towards collagenase could be explained by the high content of amino groups that allows for the sorption of the Zn^{2+} coordinated in the active site of the enzyme. Further, collagenase adsorption onto the TC10-1 outermost surface was significantly higher than in the case of chitosan ($p < 0.01$). This was expected since inclusion of free thiols in the chitosan structure improves its Zn^{2+} binding capacity[34] and thus the adsorption of collagenase. Surprisingly, collagenase adsorption was not higher on the TC5-2 surface in comparison with chitosan. Although with inclusion of a higher amount of thiol groups improved collagenase adsorption was expected, this was not the case. One possible explanation may be that a highly cross-linked structure is formed *in situ* after TC5-2 deposition *via* intra- and inter-molecular disulphide cross-linking which is promoted in the formulations with high percentages of free thiol groups due to their proximity.[53] The formation of such structure would impede the availability of the remaining free thiols and consequently the sorption capacity towards Zn^{2+}. This result is consistent with the decrease in protein adsorption after cross-linking of the PEM systems.[28]

On the other hand, adsorption of collagenase onto like-charged surfaces was different. Although the enzyme was not adsorbed onto the HA outermost layer, adsorption onto the CS containing surface occurred. This result confirms that not only electrostatic interactions, but also other non-ionic factors can

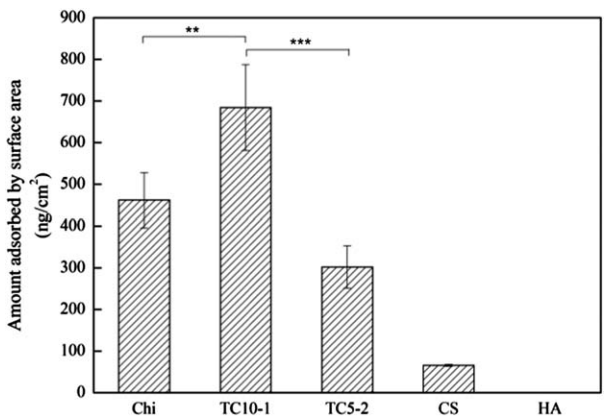

Fig. 6 Variation of collagenase adsorption (0.1 mg mL^{-1}) onto PEMs with different outermost layers in terms of amount adsorbed by the surface area. The results were obtained by extracting the data acquired by QCM-D and calculated using the Voigt model. PEM coatings comprised 10 layers in the case of polyanion and 11 in the case of the polycation outermost layer. For the PEMs terminating with polycation CS was used, whereas for those terminating with polyanion TC5-2 served as a counter polyelectrolyte. Polyelectrolytes were deposited onto gold from 0.15 M NaCl, pH 5.5 solution, using concentrations of 0.5 mg mL^{-1}. $^{**}p < 0.01$ and $^{***}p < 0.001$.

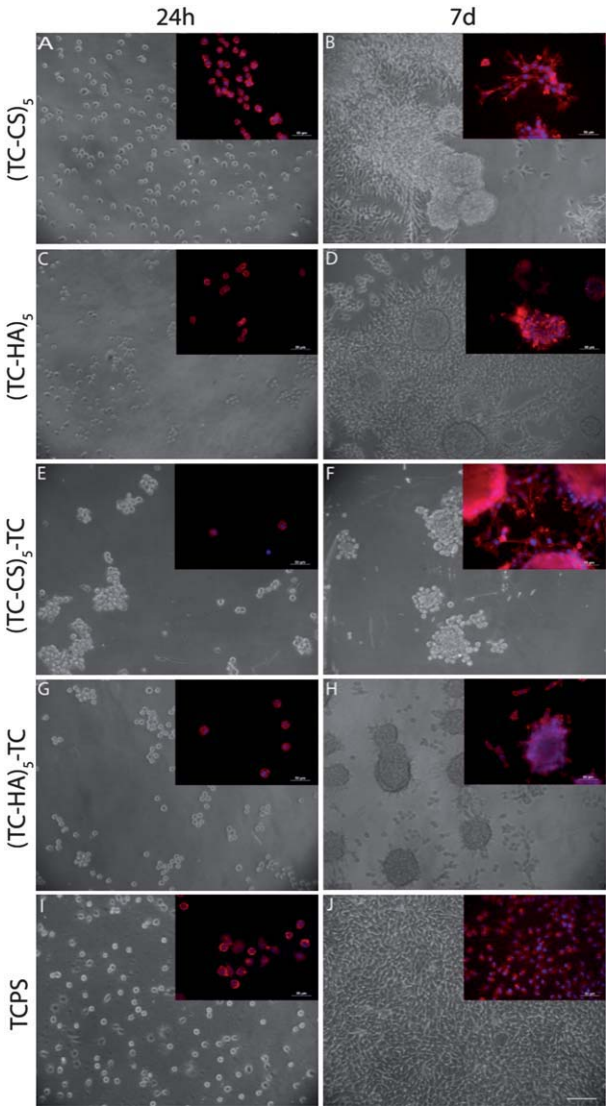

Fig. 7 Morphology of L929 cells cultured for 24 h and 7 d on (A and B) CS-terminated, (C and D) HA830-terminated, (E and F) TC terminated (TC5-2/CS system), (G and H) TC terminated (TC/HA830 system) and (I and J) TCPS (scale bar = 100 μm). Insets show fluorescence microscopy images of DAPI and phalloidin staining.

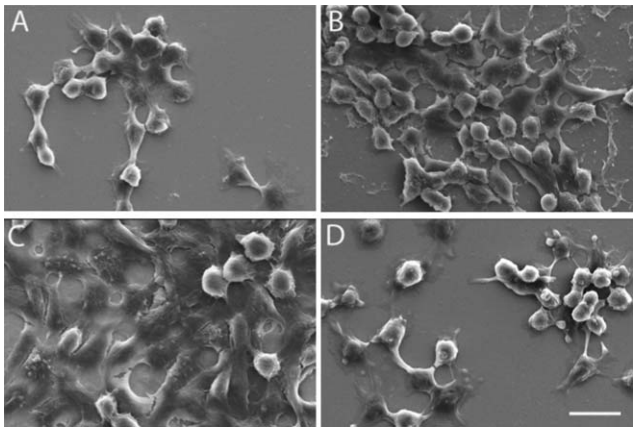

Fig. 8 Morphology of L929 cells cultured for 7 d on (A) $(TC–CS)_5$, (B) $(TC–HA)_5$, (C) $(TC–CS)_5$–TC and (D) $(TC–HA)_5$–TC (scale bar = 20 μm).

influence protein adsorption.[54] Again, GAGs-protein binding relies on multivalent interactions, some of them very difficult to measure experimentally,[55] where, besides other factors, spatial distribution of negative charges in GAGs plays an important role.[56] Also, HA displays higher negative charge (Fig. 1) which may be the explanation for stronger repulsion of the like-charged enzyme. Another factor that may influence the protein adsorption is the surface hydrophilicity. Normally, the protein attachment decreases with wettability.[57] The CS-terminated assemblies had contact angles of 54 ± 4°, whereas HA-terminated exhibited 40 ± 4°, being thus more hydrophilic.

Cell culture studies

Fibroblasts behaviour on the obtained PEM coatings was evaluated in terms of cell adhesion, morphology and cytoskeleton organisation. Bright-field images (Fig. 7) showed that after 24 h the cells adhered better on GAG-terminated coatings (Fig. 7A and C) than on thiolated chitosan (Fig. 7E and G). Moreover, the number of fibroblasts on CS-terminated coatings (Fig. 7A and B) was similar to the control surfaces (TCPS, Fig. 7I and J).

A different cell morphology was also observed as a response to the terminal layer; after 24 h, cells cultured in contact with thiolated chitosan remain round and compact (Fig. 7E and G). These results are in agreement with previously reported data about the poor cellular adhesion on the chitosan.[58,59] On the other hand, when the outermost layer is GAG (HA or CS), cells are elongated with a morphology more similar to the cells cultured on TCPS (Fig. 7A, C and I).

After one week of culture the cells tend to organise in clustered structures on the thiolated chitosan (Fig. 7F and H and 8C and D). This behaviour has been previously associated with defensive mechanisms by which cells are able to survive under unfavourable conditions.[60]

Also, the formation of the spheroid structures has already been reported for cells cultured on chitosan membranes.[58,60] Although not that pronounced, a similar behaviour was observed for the fibroblasts cultured in contact with the GAGs-terminated coatings (Fig. 7B and D and 8A and B). This result is consistent with the diffusion of the polyelectrolytes layer estimated by the QCM-D. The diffusion of the layers and its influence on the cell behaviour are also obvious for the TC-terminated coatings where the GAG layer below induces fibroblasts morphology that is similar to the one observed for the respective GAG-terminated coatings (Fig. 7 insets).

Conclusions

A detrimental effect on the healing cascade in chronic wounds induced by elevated levels of oxidative and proteolytic enzymes requires the application of surface-active dressing materials/devices to address such environments and stimulate the repair process. Within this study, thiolated chitosan conjugates were prepared and evaluated for their efficiency to control the activity of major chronic wound enzymes, such as myeloperoxidase and collagenase, and the possibility for construction of multilayered surface coatings using a layer-by-layer technique. As the inhibitory effect against myeloperoxidase was dependent on the chitosan thiolation degree, this parameter was identified as a key factor to achieve control of the enzyme activity. Further, due to their cationic properties, the obtained thiolated conjugates were successfully combined with anionic glycosaminoglycans (chondroitin sulphate and hyaluronic acid) in a sequential multilayer fashion based on electrostatic interactions to build-up continuous multilayered assemblies onto the gold surface. It was also demonstrated that the speed of the build-up process (with respect to the number of deposited layers) is promoted by the higher chitosan thiolation degree and molecular weight of glycosaminoglycans. Moreover, the proper selection of the outermost layer could be used to control the extent of collagenase adsorption onto the multilayered coatings. Chitosan-based surfaces were found to be more protein-adhesive than glycosaminoglycans. The extent of collagenase adsorption on thiolated chitosan surfaces also depends on the availability of free thiol groups able to bind the zinc in the active site of the enzyme. Finally, the multilayered structures terminating with thiolated chitosan were found to be fibroblast resistant, whereas glycosaminoglycans as the outermost layer promoted the cell proliferation. Such tuneable inhibition/adsorption of the deleterious enzymes and controlled cell proliferation applied in the wound site could bring restoration of the balance between tissue synthesis and degradation in chronic wounds necessary for healing. Further *in vivo* and evidence-based studies will reveal whether these systems could suppress the prolonged inflammation in chronic wounds and initiate the repair process.

Acknowledgements

This work was carried out under the scope of the EU projects Lidwine (contract no. FP6-026741) and Find&Bind (contract no. FP7-229292). The PhD grant BES-2008-00374 from the Spanish Ministerio de Ciencia e Innovación (MICINN) is gratefully acknowledged.

Notes and references

1 N. J. Trengove, M. C. Stacey, S. Macauley, N. Bennett, J. Gibson, F. Burslem, G. Murphy and G. Schultz, *Wound Repair Regener.*, 1999, **7**, 442–452.
2 R. Visse and H. Nagase, *Circ. Res.*, 2003, **92**, 827–839.

3 M. Rojkind, J. A. Domínguez-Rosales, N. Nieto and P. Greenwel, *Cell. Mol. Life Sci.*, 2002, **59**, 1872–1891.
4 L. G. Ovington, *Clin. Dermatol.*, 2007, **25**, 33–38.
5 R. J. Morin and N. L. Tomaselli, *Clin. Plast. Surg.*, 2007, **34**, 643–658.
6 J. S. Boateng, K. H. Matthews, H. N. E. Stevens and G. M. Eccleston, *J. Pharm. Sci.*, 2008, **97**, 2892–2923.
7 B. S. Atiyeh, M. Costagliola, S. N. Hayek and S. A. Dibo, *Burns*, 2007, **33**, 139–148.
8 D. Falconnet, G. Csucs, H. Michelle Grandin and M. Textor, *Biomaterials*, 2006, **27**, 3044–3063.
9 R. Hong, N. O. Fischer, A. Verma, C. M. Goodman, T. Emrick and V. M. Rotello, *J. Am. Chem. Soc.*, 2004, **126**, 739–743.
10 Z. Gu, M. Kaul, B. Yan, S. J. Kridel, J. Cui, A. Strongin, J. W. Smith, R. C. Liddington and S. A. Lipton, *Science*, 2002, **297**, 1186–1190.
11 O. A. Andreassen, A. Dedeoglu, P. Klivenyi, M. F. Beal and A. I. Bush, *NeuroReport*, 2000, **11**, 2491–2493.
12 P. Van Antwerpen, K. Z. Boudjeltia, S. Babar, I. Legssyer, P. Moreau, N. Moguilevsky, M. Vanhaeverbeek, J. Ducobu and J. Nève, *Biochem. Biophys. Res. Commun.*, 2005, **337**, 82–88.
13 H. Orelma, I. Filpponen, L.-S. Johansson, J. Laine and O. J. Rojas, *Biomacromolecules*, 2011, **12**, 4311–4318.
14 D. S. Kommireddy, S. M. Sriram, Y. M. Lvov and D. K. Mills, *Biomaterials*, 2006, **27**, 4296–4303.
15 K. Ariga, J. P. Hill and Q. Ji, *Phys. Chem. Chem. Phys.*, 2007, **9**, 2319–2340.
16 C. J. Detzel, A. L. Larkin and P. Rajagopalan, *Tissue Eng., Part B: Rev.*, 2011, **17**, 101–113.
17 Y. Liu, S. Cai, X. Z. Shu, J. Shelby and G. D. Prestwich, *Wound Repair Regener.*, 2007, **15**, 245–251.
18 M. Proctor, K. Proctor, X. Z. Shu, L. D. McGill, G. D. Prestwich and R. R. Orlandi, *Am. J. Rhinol.*, 2006, **20**, 206–211.
19 M. B. Brown and S. A. Jones, *J. Eur. Acad. Dermatol. Venereol.*, 2005, **19**, 308–318.
20 C. Scordilis-Kelley and J. G. Osteryoung, *J. Phys. Chem.*, 1996, **100**, 797–804.
21 H. Ueno, H. Yamada, I. Tanaka, N. Kaba, M. Matsuura, M. Okumura, T. Kadosawa and T. Fujinaga, *Biomaterials*, 1999, **20**, 1407–1414.
22 A. Domard, *Int. J. Biol. Macromol.*, 1987, **9**, 98–104.
23 A. Bernkop-Schnürch, H. Zarti and G. F. Walker, *J. Pharm. Sci.*, 2001, **90**, 1907–1914.
24 A. Bernkop-Schnürch, C. E. Kast and D. Guggi, *J. Controlled Release*, 2003, **93**, 95–103.
25 M. D. Hornof, C. E. Kast and A. Bernkop-Schnürch, *Eur. J. Pharm. Biopharm.*, 2003, **55**, 185–190.
26 C. Capeillère-Blandin, *Biochem. J.*, 1998, **336**(Pt 2), 395–404.
27 H. E. Van Wart and D. R. Steinbrink, *Anal. Biochem.*, 1981, **113**, 356–365.
28 G. V. Martins, E. G. Merino, J. F. Mano and N. M. Alves, *Macromol. Biosci.*, 2010, **10**, 1444–1455.
29 A. Bernkop-Schnürch, M. Hornof and T. Zoidl, *Int. J. Pharm.*, 2003, **260**, 229–237.
30 D. R. Yager, R. A. Kulina and L. A. Gilman, *Int. J. Low. Extrem. Wounds*, 2007, **6**, 262–272.
31 S. J. Nicholls and S. L. Hazen, *J. Lipid Res.*, 2009, **50**, S346–S351.
32 J. Fisher and S. Mobashery, *Cancer Metastasis Rev.*, 2006, **25**, 115–136.
33 B. G. Rao, *Curr. Pharm. Des.*, 2005, **11**, 295–322.
34 I. Bravo-Osuna, C. Vauthier, A. Farabollini, G. Millotti and G. Ponchel, *J. Nanopart. Res.*, 2008, **10**, 1293–1301.
35 D. G. Castner, K. Hinds and D. W. Grainger, *Langmuir*, 1996, **12**, 5083–5086.
36 C. Picart, J. Mutterer, L. Richert, Y. Luo, G. D. Prestwich, P. Schaaf, J. C. Voegel and P. Lavalle, *Proc. Natl. Acad. Sci. U. S. A.*, 2002, **99**, 12531–12535.
37 H. Zhang, A. Qadeer and W. Chen, *Biomacromolecules*, 2011, **12**, 1428–1437.
38 T. I. Croll, A. J. O'Connor, G. W. Stevens and J. J. Cooper-White, *Biomacromolecules*, 2006, **7**, 1610–1622.
39 L. Richert, A. J. Engler, D. E. Discher and C. Picart, *Biomacromolecules*, 2004, **5**, 1908–1916.
40 J. C. Paulson, O. Blixt and B. E. Collins, *Nat. Chem. Biol.*, 2006, **2**, 238–248.
41 S. Fukui, T. Feizi, C. Galustian, A. M. Lawson and W. Chai, *Nat. Biotechnol.*, 2002, **20**, 1011–1017.
42 K.-S. Ko, F. A. Jaipuri and N. L. Pohl, *J. Am. Chem. Soc.*, 2005, **127**, 13162–13163.
43 C. Porcel, P. Lavalle, G. Decher, B. Senger, J. C. Voegel and P. Schaaf, *Langmuir*, 2007, **23**, 1898–1904.
44 P. Lisboa, A. Valsesia, P. Colpo, D. Gilliland, G. Ceccone, A. Papadopoulou-Bouraoui, H. Rauscher, F. Reniero, C. Guillou and F. Rossi, *Appl. Surf. Sci.*, 2007, **253**, 4796–4804.
45 B. Genorio, T. He, A. Meden, S. Polanc, J. Jamnik and J. M. Tour, *Langmuir*, 2008, **24**, 11523–11532.
46 D. S. Salloum and J. B. Schlenoff, *Biomacromolecules*, 2004, **5**, 1089–1096.
47 A. Reisch, J.-C. Voegel, E. Gonthier, G. Decher, B. Senger, P. Schaaf and P. J. Mésini, *Langmuir*, 2009, **25**, 3610–3617.
48 J. V. Edwards and P. S. Howley, *J. Biomed. Mater. Res., Part A*, 2007, **83A**, 446–454.
49 B. Cullen, R. Smith, E. McCulloch, D. Silcock and L. Morrison, *Wound Repair Regener.*, 2002, **10**, 16–25.
50 M. D. Bond and H. E. Van Wart, *Biochemistry*, 1984, **23**, 3085–3091.
51 A. K. Bajpai, *Polym. Int.*, 2007, **56**, 231–244.
52 F. Bernsmann, B. Frisch, C. Ringwald and V. Ball, *J. Colloid Interface Sci.*, 2010, **344**, 54–60.
53 I. Bravo-Osuna, D. Teutonico, S. Arpicco, C. Vauthier and G. Ponchel, *Int. J. Pharm.*, 2007, **340**, 173–181.
54 R. E. Hileman, J. R. Fromm, J. M. Weiler and R. J. Linhardt, *BioEssays*, 1998, **20**, 156–167.
55 I. Pashkuleva and R. L. Reis, *J. Mater. Chem.*, 2010, **20**, 8803–8818.
56 J. J. Valle-Delgado, M. Alfonso-Prieto, N. S. de Groot, S. Ventura, J. Samitier, C. Rovira and X. Fernàndez-Busquets, *FASEB J.*, 2010, **24**, 4250–4261.
57 P. Roach, D. Farrar and C. C. Perry, *J. Am. Chem. Soc.*, 2005, **127**, 8168–8173.
58 A.-P. Zhu and N. Fang, *Biomacromolecules*, 2005, **6**, 2607–2614.
59 P. M. Lopez-Perez, A. P. Marques, R. M. P. da Silva, I. Pashkuleva and R. L. Reis, *J. Mater. Chem.*, 2007, **17**, 4064–4071.
60 G.-S. Huang, L.-G. Dai, B. L. Yen and S.-h. Hsu, *Biomaterials*, 2011, **32**, 6929–6945.

